Title
A Solid-State 199Hg NMR Study of Mercury Halides

Journal
Journal of Molecular Structure, 987

Authors
Taylor, Robert E
Bai, Shi
Dybowski, Cecil

Publication Date
2011

DOI
10.1016/j.molstruc.2010.12.013

Peer reviewed

A Solid-State ^{199}Hg NMR Study of Mercury Halides

R. E. Taylor[1]*, Shi Bai[2], and C. Dybowski[2]

[1]Department of Chemistry and Biochemistry
University of California, Los Angeles
Los Angeles, CA 90095-1569 USA

and

[2]Department of Chemistry and Biochemistry
University of Delaware
Newark, DE 19716-2522 USA

*Corresponding author: R. E. Taylor
Email address: taylor@chem.ucla.edu

Abstract:

The principal elements of the ^{199}Hg chemical-shift (CS) tensors of the mercuric halides (HgX_2, X = F, Cl, Br, and I) and the mercurous halides (Hg_2X_2, X = F and Cl) were determined from spectra of static polycrystalline powders and from magic-angle spinning (MAS) spectra. The CS tensors of both $HgCl_2$ and Hg_2Cl_2 are axially symmetric ($\eta = 0$) within experimental error, differing from literature reports of η=0.12 and η=0.14, respectively. The principal elements of the axially symmetric CS tensor in $HgBr_2$ were also measured using a static sample, and the wideline spectra of HgF_2 and HgI_2 (red polymorph) give chemical-shift tensors that suggest, within experimental error, that the mercury sits in sites of cubic symmetry. The ^{199}Hg CS tensor for Hg_2F_2 is asymmetric. Experiments with static polycrystalline samples may allow the determination of the elements of the ^{199}Hg CS tensors even when MAS fails to completely average the dipolar coupling of the spin-½ ^{199}Hg and the quadrupolar halide nucleus.

Key Words:

^{199}Hg NMR; mercury; halide; chemical shielding; chemical-shift anisotropy.

Introduction

Nuclear magnetic resonance (NMR) studies provide insights into the electronic and geometric structures of molecules, particularly through the analysis of the complete chemical-shift (CS) tensor available from the NMR spectroscopy of solids. The experimental challenge of these measurements on heavy metals such as mercury arises from the typically large chemical-shift dispersion (often several thousands of parts per million) and long spin-lattice relaxation times [1,2]. One method of sensitivity enhancement that is often used in solid-state ^{199}Hg NMR studies is cross-polarization (CP) from abundant spins such as protons [3-5]. Cross-polarization from the abundant ^{19}F spins might be useful in investigations of the fluorinated halides (assuming the availability of appropriate spectrometer hardware), but such a technique is not applicable to the other halides due to the lack of an abundant spin system such as protons or fluorine atoms that have a high magnetogyric ratio. Direct polarization techniques, with their limitations, must be used to obtain these spectra. Another common technique to increase sensitivity in spectra of solids is magic-angle spinning (MAS) [1,2]. However, even that technique is of limited use, as the dipolar coupling between the spin-½ ^{199}Hg and the quadrupolar halide nucleus does not completely average to zero under MAS [6].

Mercury forms both mercurous(I) and mercuric(II) halides. In the solid state, the mercurous compounds are typically linear or near-linear species containing discrete metal-metal bonds of Hg_2^{2+} [7]. The mercuric structures are also typically linear, though HgF_2 has a cubic CaF_2-type structure and HgI_2 displays a diversity of structures and colors [8]. Given that the ^{199}Hg spin-½ isotope has a natural abundance of 16.87% and a receptivity of 5.89 relative to ^{13}C [9], both series of halides are amenable to study by ^{199}Hg NMR spectroscopy.

Mercury halides are interesting not just as representative structures of solids of heavy transition metals, but also because the materials appear in the environment. That mercury is frequently toxic and an environmental hazard is a well-known fact [10,11]. One source of mercury in the environment is emissions from coal combustion and waste incineration [12]. As mercury is highly volatile, it is typically emitted from such combustion processes in flue gases either as elemental mercury or as oxidized compounds, including $HgCl_2$. Mercury "is considered a global pollutant due to its ability to undergo long distance transport in the atmosphere" [13] and is consequently monitored. Periodically, gaseous mercury that has been exhausted into the atmosphere is removed from the troposphere in the Artic and Antarctic, accumulating on snow and ice surfaces. It is thought that elemental mercury formed in this way can react with halogen radicals to form species such as $HgBr_2$ and $HgCl_2$ in the environment [14-16]. The ingestion of mercury may produce biological structures containing mercury in various forms. Indeed, the ^{199}Hg NMR of Hg(II) incorporated as a bioprobe in metalloproteins and enzymes has been reported [10,17-19].

Aside from the potential dangers of mercury-containing materials, the mercury halides also show technological promise. Mercuric iodide is used as a room-temperature X- and γ-ray detector [20,21] and $HgBr_xI_{1-x}$ has been investigated as a photodetector [22]. Acousto-optical devices containing mercury compounds are used in military, space, and commercial applications, including the detection of targets and of chemical and biological agents. Hg_2Cl_2 and Hg_2Br_2 have suitable properties for such devices in an imaging system operating in the long-wavelength infrared region of the atmospheric transmission window [23].

MAS techniques have been previously used to measure the principal elements of the ^{199}Hg CS tensors of both $HgCl_2$ [24] and Hg_2Cl_2 [7]. However, recent work [26] has shown that the CS tensor of $HgCl_2$ appears to be, within experimental error, axially symmetric ($\eta = 0$), differing from the literature value of $\eta = 0.12$ obtained from an analysis of MAS data [24]. An attempt to use the ^{199}Hg MAS spectrum of $HgBr_2$ [25] to determine the principal components of the ^{199}Hg CS tensor was reported to be unsuccessful due to the coupling to the ^{79,81}Br. The goal of the present work is to measure the principal elements of the ^{199}Hg CS tensors of these, and other, mercury halides using wideline NMR techniques on solid, static samples. Previous work [26] has shown that interactions with solvent molecules alter the structure and consequently the CS tensor in solution.

In the case of Hg_2Cl_2, the principal components of the ^{199}Hg CS tensor may be compared with those previously determined by MAS techniques. The experimental results are also discussed in terms of various theoretical studies. With current calculational capabilities, theoretical studies of Hg in the solid state usually predict only qualitative trends. For example, one such study of $HgCl_2$ [25] yielded calculated CS spans that were consistently larger than those observed experimentally. Hostettler and Schwarzenbach [8] expressed regret "that *ab initio* quantum mechanical calculations are not yet available to elucidate the preferred bonding modes of these heavy atoms". The experimental results of the present work for these mercury halide series provide theorists with the opportunity to further develop state-of-the-art calculations and to move from qualitative agreement to quantitative. After all, such a comparison of experimental spectroscopic parameters with calculated parameters provides a less-empirical means of understanding the connection between NMR parameters and the electronic state of the material, which is the focus of chemical inquiry [26].

Experimental

The ^{199}Hg NMR data were acquired at a magnetic field strength of 7.05 T using Bruker Avance 300 and MSL 300 spectrometers. The NMR data are referenced relative to the position of the resonance of dimethylmercury at 0 ppm, using the external secondary reference [27] of a 1.0 M sample of $HgCl_2$ in d_6-DMSO at -1501.6 ppm. The static polycrystalline samples were examined with a standard Bruker X-nucleus wideline probe with a 5-mm solenoid coil. The ^{199}Hg $\pi/2$ pulse width was 3.75 μs for these experiments. In cases in which the powder spectra were broad, spectra were obtained by the variable offset cumulative spectra (VOCS) method [28]. MAS spectra of polycrystalline samples were acquired with a standard Bruker 4-mm MAS probe, using a ^{199}Hg $\pi/2$ pulse width of 4 μs. The significantly long spin-relaxation times of these mercury materials in the solid state were measured by the saturation-recovery technique [29]. Temperature measurements were calibrated with the chemical shift of solid lead nitrate for both static [30] and MAS [31-33] experiments.

Simulation of chemical-shift powder patterns of static samples and of MAS spectra of spinning samples using the Herzfeld-Berger technique [34] were performed with the solids simulation package ("solaguide") in the TopSpin (Version 2.1) NMR software program from Bruker BioSpin.

Results and Discussion

The geometric arrangement of the atoms within a molecule is determined by the electronic bonding. The nature of the electronic bonding determines the shieldings of NMR-active nuclei within the molecule. The mercuric compounds frequently adopt a linear geometry with a coordination number of two, i.e., two ligands forming covalent bonds linearly arranged around a central mercury atom. This total number of strong covalent bonds is often referred to as the "characteristic coordination number". Often, however, there are secondary bonds to additional neighboring atoms that are within the sum of the ligand and mercury van der Waals radii [35]. Thus, the total number of bonding contacts is referred to as the "effective coordination number". Mercuric compounds are usually described as having a 2 + *n* coordination, with *n* typically being 3-5 [36]. It is this combination of covalent and secondary bonds that determines the chemical shielding within the compounds, as well as other physical properties such as melting and boiling points.

The mercurous halides [37,38] and the mercuric halides [14,36,39] have been the subject of theoretical studies. For such studies, the importance of including relativistic effects on the electronic structure of mercury compounds has been known for some time [36,39,40]. The fact that electrons may be moving at appreciable fractions of the speed of light requires that relativistically invariant calculations such as the zeroth-order regular approximation (ZORA) with density functional theory (DFT) [25,41-43] be used to calculate the ^{199}Hg NMR chemical shielding.

Mercuric Halides

HgF_2 has a CaF_2 (fluorite) structure [8,39] with a coordination number of 8, very different from the other mercuric halides. The mercury atom is located at the center of a cubic cell with eight fluorine atoms at the corners. The Hg-F distance is 246 pm [36]. The ^{199}Hg wideline spectrum of a static sample of HgF_2 at ambient temperature is shown in Figure 1. The cubic crystal symmetry is consistent with an isotropic chemical shift tensor. The resonance has a relatively narrow line width of 2.8 kHz, dominated by ^{199}Hg-^{19}F dipolar broadening.

For the fluorite structure of HgF_2, Donald *et al*. [39] argue that this structural preference, at least to some degree, results from the difference of the ratio of the metal cation radius to that of the fluoride ion, as compared to the other halide ions. They note that the radius of the Hg^{2+} cation (~114 pm) is relatively close to that of the Ca^{2+} cation (~112 pm). Even though the electronegativity difference ($\Delta\chi$) between the metal and the fluoride is smaller for mercury than it is for calcium, "the ratio of the Hg^{2+} and F^- radii and other packing forces favor the fluorite structure, and overcompensate for the destabilizing influence of the decrease in $\Delta\chi$ on going from Ca to Cd to Hg". Their calculations suggest that, as more fluorides coordinate to the mercury, an "ionic switch is turned on". Although the way this "ionic progression" occurs is "not completely understood", they note that in dimers, the mercury and the bridging fluorides are more ionic than the same centers in the monomer.

In contrast, the mercuric chloride, bromide, and iodide have less of a difference in electronegativity between the metal and halide atoms than the fluoride. As a result, the ionicity of these compounds is diminished, leading to the observation that $HgCl_2$ and

$HgBr_2$ are molecular solids. The red α-HgI_2 structure is not strictly molecular but "exhibits layers of edge-sharing HgI_4 tetrahedra" [36]. An overview of the physical properties of the mercuric (II) halides is given in Table I.

An examination of the reported crystal structure of $HgCl_2$ suggests that, in the solid state, the $HgCl_2$ molecule may be considered linear [44]. The Cl-Hg-Cl angle is 178.9(5)°, with the two Hg-Cl distances slightly inequivalent at 228.4 pm and 230.1 pm. The crystal is orthorhombic with a space group of *Pnma*. Each mercury atom has four nonbonded interactions with chlorines on adjacent molecules (with distances ranging from 334 to 363 pm).

The ^{199}Hg variable offset cumulative spectrum (VOCS) [28] of static $HgCl_2$, shown in Figure 2 together with a simulation, has been previously published [25]. The ^{199}Hg MAS spectrum of polycrystalline $HgCl_2$ is shown in Figure 3A. The smooth lines in Figure 3 represent a simulation [34] to extract the principal components of the chemical-shift tensor from the pattern of sidebands. The resulting CS parameters are given in Table II. This finding is materially different from the results reported by Bowmaker *et al.* [7, 24]. The ^{199}Hg spin-lattice relaxation time at ambient temperature was 51 s.

$HgBr_2$ forms a crystal with linear Br-Hg-Br structures with a space group of $Cmc2_1$ [2]. The coordination is 2 + 4, with two Hg-Br bond distances of 248 pm and four bromine atoms at a distance of 323 pm. The ^{199}Hg NMR spectrum of a static sample of $HgBr_2$ is shown in Figure 4. The ^{199}Hg spin-lattice relaxation time at ambient temperature is 200 s. The CS tensor parameters are given in Table II. The ^{199}Hg MAS spectrum of $HgBr_2$ in Figure 3B illustrates that the Herzfeld-Berger [34] simulation cannot be successfully used to extract the CSA parameters because the dipolar couplings between the spin-½ ^{199}Hg and the quadrupolar bromine nuclei are not completely averaged to zero under MAS [6]. Harris and co-workers noted a "failure to obtain good quality ^{199}Hg spectra for X = Br, I" [24] and attributed the severe broadening of the ^{199}Hg resonance to "unresolved coupling to the ^{79}Br, ^{81}Br nuclei" [7]. However, the very large chemical-shift anisotropy in the static spectrum allows the CS tensor parameters to be extracted from the simulation.

The red polymorph of HgI_2 has a coordination number of 4, forming corner-linked HgI_4 tetrahedra [8]. The space group is $P4_2/nmc$ with four Hg-I distances of 278.3 pm [45]. The ^{199}Hg NMR spectrum of a static sample of the red polymorph of HgI_2 is shown in Figure 5. The ^{199}Hg spin-lattice relaxation time at ambient temperature is 62 s. The spectrum does not clearly show spectral features expected of the powder pattern due to chemical shielding. The full width at half maximum (FWHM) of the spectral resonance is 24.2 kHz (*ca*. 464 ppm), which places an upper limit on the chemical-shift dispersion. The ^{199}Hg MAS spectrum is shown in Figure 3C. The FWHM of the isotropic peak is *ca*. 12 kHz, arising from the residual dipolar coupling to the quadrupolar iodine nuclei that is not averaged by the MAS. The ^{199}Hg line widths of the isotropic peaks in the MAS spectra of the mercuric halides increase with the atomic weight of the halide as well as the quadrupolar moment of the halide. The NMR properties of the mercury isotopes as well as the halides are given in Table III.

Mercurous Halides

The crystals of the mercurous halides have a linear X-Hg-Hg-X unit. The mercury atom lies in a distorted octahedral environment. There is a short Hg-X bond and a

slightly larger distance to the four next-nearest-neighbor halides. The Hg-X distances for the mercurous halides are given in Table IV.

The ^{199}Hg NMR spectrum of a static sample of Hg_2F_2 is shown in Figure 6. The parameters derived from the simulation of the CS tensor are given in Table II. In contrast to the other mercurous and mercuric halides, the Hg_2F_2 does not display axially symmetric shielding, likely resulting from interactions with the four next nearest neighbor (secondary) fluorine atoms. In addition to the CS tensor, the simulation in Figure 6 also includes a co-linear heteronuclear dipolar interaction of 14.8 kHz between the ^{19}F and the ^{199}Hg nuclei. Dipolar interactions with the four secondary fluorine atoms and scalar interactions are ignored in the simulation.

Kleier and Wadt [37] used theoretical calculations to investigate whether "the dimer of HgCl (HgF) {is} best described by a covalent linkage between the mercury atoms of the HgCl (HgF) monomers or by a largely electrostatic interaction between HgCl (HgF) dipoles". Although noting that "all the mercurous halides are known to crystallize in molecular lattices of linear X-Hg-Hg-X molecules" [46-48], their focus on monomers and dimers avoided the "complications due to crystal-packing forces". Even though the Hg-X bond is polar in the monomer, the "moderately strong covalent bond between the mercury atoms dictates a linear structure (X-Hg-Hg-X) for both fluoride and chloride".

Kaupp and von Schnering [38] also have investigated the Hg-Hg bond through computation. They concluded that, in the gas phase, the mercuric halide (HgX_2) is favored in spite of "a slight relativistic stabilization of the Hg-Hg bond" in the mercurous halide (Hg_2X_2). "Intrinsic condensed-phase interactions are responsible for the stability of Hg-Hg cations."

The ^{199}Hg NMR spectrum of a static sample of Hg_2Cl_2 is shown in Figure 7. The ^{199}Hg spin-lattice relaxation time at ambient temperature is 94 s. The parameters derived from the simulation of the CS tensor are given in Table II. Whether using the data from the static sample or from the MAS experiment (Figure 8), the CS tensor of Hg_2Cl_2 appears axially symmetric ($\eta = 0$), within experimental error, differing from the literature value of $\eta = 0.14$ obtained from an analysis of MAS data [7]. This reported value of $\eta = 0.14$ obtained from an analysis of MAS data of Hg_2Cl_2 is quite similar to $\eta = 0.12$ for $HgCl_2$ [24]. In that study [24], Harris and co-workers noted that accuracy was limited by both high noise levels and the required baseline corrections arising from the use of a MAS probe over large spectral widths. The use of a wideline probe with the VOCS technique in the present study addresses the baseline issue.

Conclusions

The principal values of the ^{199}Hg CS tensors of several mercury halides were obtained using wideline NMR techniques on static samples. Both $HgCl_2$ and Hg_2Cl_2 were found to have axially symmetric CS tensors, within experimental error, differing from previous literature results obtained from MAS measurements [7,24]. In agreement with an earlier report [7], analysis of the spinning sidebands from a ^{199}Hg MAS experiment with $HgBr_2$ could not be properly analyzed due to the strong dipolar coupling to the quadrupolar ^{79,81}Br. However, the principal values of the ^{199}Hg CS tensor in $HgBr_2$ were obtained using wideline NMR techniques on a static sample. In most cases save for HgF_2 (which has cubic symmetry) and HgI_2, the anisotropy of the chemical-shift tensor is well over 1000 ppm. The ^{199}Hg wideline spectra for both HgF_2 and HgI_2 (red polymorph) suggest

that the mercury is in sites of cubic symmetry, at least within experimental error. Hg_2F_2 is markedly different, in that a nonaxial CS tensor is obtained from the wideline spectrum.

Acknowledgment

This material is based upon work supported by the National Science Foundation under Equipment Grant # DMR-9975975. CRD acknowledges support of NMR studies by the National Science Foundation under Grants CHE-0411790 and CHE-0956006.

References

[1] R. Siegel, T. T. Nakashima, and R. E. Wasylishen, *J. Phys. Chem. B* **108** (2004), 2218-2226.

[2] I. Hung, A. J. Rossini, and R. W. Schurko, *J. Phys. Chem. A* **108** (2004), 7112-7120.

[3] R. K. Harris and A. Sebald, *Magn. Reson. Chem*. **25** (1987), 1058-1062.

[4] K. Eichele, S. Kroeker, G. Wu, and R. E. Wasylishen, *Solid State NMR* **4** (1995), 295-300.

[5] J. M. Hook, P. A. W. Dean, and L. C. M. van Gorkom, *Magn. Reson. Chem*. **33** (1995), 77-79.

[6] D. L. Bryce and G. D. Sward, *Magn. Reson. Chem*. **44** (2006), 409-450.

[7] G. A. Bowmaker, R. K. Harris, and D. C. Apperley, *Inorg. Chem*. **38** (1999), 4956-4962.

[8] M. Hostettler and D. Schwarzenbach, *C. R. Chimie* **8** (2004), 147-156.

[9] R. K. Harris, E. D. Becker, S. M. Carbral De Menezies, R. Goodfellow, and P. Granger, *Pure Appl. Chem*. **73** (2001), 1795-1818.

[10] O. Iranzo, P. W. Thulstrup, S-b. Ryu, L. Hemmingsen, and V. L. Pecoraro, *Chem. Eur. J*. **13** (2007), 9178-9190.

[11] J. Liu, J-Z. Shi, L-M. Yu, R. A. Goyer, and M. P. Waalkees, *Exp. Bio. Med*. **233** (2008), 810-817.

[12] R. R. Kotdawala, N. Kazantis, and R. W. Thompson, *Environ. Chem*. **4** (2007), 55-64.

[13] Q. Wan, X. Feng, J. Lu, W. Zheng, X. Song, S. Han, and H. Xu, *Environ. Res*. **109** (2009), 201-206.

[14] N. B. Balabanov and K. A. Peterson, *J. Chem. Phys*. **119** (2003), 12271-12278.

[15] W. H. Schroeder, K. G. Anlauf, L. A. Barrie,J. Y. Lu, A Steffen, D. R. Schneeberger, and T. Berg, *Nature* **394** (1998), 331-332.

[16] S. E. Lindberg, S. Brooks, C.-J. Lin, K. J. Scott, M. S. Landis, R. K. Stevens, M. Goodsite, and A. Richter, *Environ. Sci. Technol*. **36** (2002), 1245-1256.

[17] S. P. Watton, J. G. Wright, F. M. MacDonnell, J. W. Bryson, M. Sabat, and T. V. O'Halloran, *J. Am. Chem. Soc*. **112** (1990), 2824-2826.

[18] L. M. Utschig, J. W. Bryson, and T. V. O'Halloran, *Science* **268** (1995), 380-385.

[19] L. M. Utschig, T. Baynard, C. Strong, and T. V. O'Halloran, *Inorg. Chem*. **36** (1997), 2926-2927.

[20] B. Steiner, L. van dan Berg, and U. Laor, *J. Appl. Phys*. **86** (1999), 4677-4687.

[21] M. Schieber, H. Hermon, A. Zuck, A. Vilensky, L. Melekhov, R. Shatunovsky, E. Meerson, and H. Saado, *Nucl. Inst. Meth. Phys. Res. A* **458** (2001), 41-46.

[22] R. Farrell, F. Olschner, K. Shah, and M. R. Squillante, *Nucl. Inst. Meth. Phys. Res. A* **387** (1997), 194-198.

[23] J-S. Kim, S. B. Trivedi, J. Soos, N. Gupta, and W. Palosz, *J. Crys. Growth* **310** (2008), 2457-2463.

[24] G. A. Bowmaker, A. V. Churakov, R. K. Harris, and S-W. Oh, *J. Organomet. Chem*. **550** (1998), 89-99.

[25] R. E. Taylor, C. T. Carver, R. E. Larsen, O. Dmitrenko, S. Bai, and C. Dybowski, *J. Mol. Struct*. **930** (2009), 99-109.

[26] C. M. Widdifeld and R. W. Schurko, Concepts Magn. Reson. A **34** (2009), 91-123.

[27] M. A. Sens, N. K. Wilson, P. D. Ellis, and J. D. Odom, *J. Magn. Reson*. **19** (1975), 323-336.

[28] D. Massiot, I. Farnan, N. Gautier, D. Trumeau, A. Trokiner, and J. P. Coutures, *Solid State NMR* **4** (1995), 241-248.

[29] T. C. Farrar and E. D. Becker, *Pulse and Fourier Transform NMR, Introduction to Theory and Methods*, Academic Press, New York, 1971, p. 20-22.

[30] P. A. Beckman and C. Dybowski, *J. Magn. Res* **146** (2000), 379-380.

[31] A. Bielecki and D. P. Burum, *J. Magn. Reson. A* **116** (1995), 215-220.

[32] G. Neue and C. Dybowski, Solid *State NMR* **7** (1997), 333-336.

[33] R. E. Taylor, *Concepts Magn. Reson. A* **22** (2004), 79-89.

[34] J. Herzfeld and A. E. Berger, *J. Chem. Phys*. **73** (1980), 6021-6030.

[35] A. Bondi, *J. Phys. Chem*. **68** (1964), 441-451.

[36] M. Kaupp and H. G. von Schnering, *Inorg. Chem*. **33** (1994), 2555-2564.

[37] D. A. Kleier and W. R. Wadt, *J. Am. Chem. Soc*. **102** (1980), 6909-6913.

[38] M. Kaupp and H. G. von Schnering, *Inorg. Chem.* **33** (1994), 4179-4185.

[39] K. J. Donald, M. Hargittai, and R. Hoffmann, *Chem. Eur. J*. **15** (2009), 158-177.

[40] P. P. Singh, *Phys. Rev. B* **49** (1994), 4954-4958.

[41] S. K. Wolff, T. Ziegler, E. van Lenthe and E. J. Baerends, *J. Chem. Phys*. **110** (1999), 7689-7698.

[42] J. Autschbach and T. Ziegler, *J. Am. Chem. Soc*. **123** (2001), 3341-3349.

[43] J. Jokisaari, S. Järvinen, J. Autschbach, and T. Ziegler, *J. Phys. Chem. A* **106** (2002), 9313-9318.

[44] V. Subramanian and K. Seff, *Acta Cryst*. **B36** (1980), 2132-2135.

[45] G. A. Jeffrey and M. Vlasse, *Inorg. Chem*. **6** (1967), 396-399.

[46] D. Grdenić and C. Djordjević, *J. Chem. Soc*. (1956), 1316-1319.

[47] E. Dorm, *J. Chem. Soc. D: Chem. Comm*. (1970), 466-467.

[48] R. J. Havighurst, *J. Am. Chem. Soc*. **48** (1926), 2113-2125.

[49] R. K. Harris and B. E. Mann, *NMR and the Periodic Table*, Academic Press, New York, 1978, p. 268.

Tables

Table I. Physical Properties of Mercuric(II) Halides

Compound	^{199}Hg δ_{iso}, 1M in d_6-DMSO	^{199}Hg δ_{iso}, solid state	Melting Point (°C)	Boiling Point (°C)	Enthalpy of Vaporization ΔH_{vap}^{298} (kJ/mol)	Hg-X Distance, Solid-state (pm)
HgF_2	---[a]	-2826	645(dec)[b]	647[b]	92.0[b]	8 x 246[b]
$HgCl_2$	-1501.6	-1624	277[b]	304[b]	58.9[b]	2 x 225[b] 2 x 334[b] 2 x 363[b]
$HgBr_2$	-2067.4	-2352	245[b]	319[b]	59.2[b]	2 x 248[b] 4 x 323[b]
HgI_2	-3106[c]	~-3046	257[b]	354[b]	59.2[b]	2 x 262[b] 4 x 351[b]

[a]HgF_2 is insoluble in DMSO. A ^{199}Hg chemical of -2387 ppm was measured with 1 mL of a 1 M solution in D_2O with 200 μL of 67% nitric acid added.
[b]From Ref. 36
[c]From Ref. 49

Table II. ^{199}Hg NMR Parameters of Solid Mercury Halides								
Compound	δ_{11}[c] (ppm)	δ_{22}[c] (ppm)	δ_{33}[c] (ppm)	δ_{iso} (ppm)	ζ_{csa}[d] (ppm)	η[e]	Ω[f] (ppm)	κ[g]
HgF_2 Static[a]	-2826	-2826	-2826	-2826	0	--	0	--
$HgCl_2$ Static[a]	-385	-385	-4104	-1625	-2479	0.00	3719	1.00
$HgCl_2$ MAS[a]	-409	-418	-4045	-1624	-2421	0.004	3636	1.00
$HgBr_2$ Static[a]	-1945	-1945	-3293	-2394	-899	0.00	1348	1.00
HgI_2 Static[a]	-3131	-3131	-3131	-3131	0	--	0	--
Hg_2F_2 Static[b]	596	-2383	-3110	-1632	2228	0.33	3706	-0.61
Hg_2Cl_2 Static[a]	236	236	-3452	-993	-2511	0.00	3688	1.00
Hg_2Cl_2 MAS[a]	202	200	-3566	-1055	-2511	0.00	3767	1.00

[a]Chemical shifts referenced to neat dimethylmercury by use of 1 M $HgCl_2$ in d_6-DMSO as a secondary reference assigned as -1501.6 ppm (Ref. 27).
[b]Chemical shifts referenced to neat dimethylmercury by use of $[N(Et)_4]Na[Hg(CN)_4]$ as a secondary reference assigned as -434 ppm (Ref. 4).
[c]Estimated uncertainty, ± 10 ppm.
[d]$\zeta_{csa} = \delta_{33} - \delta_{iso}$.
[d]$\eta = (\delta_{22} - \delta_{11})/\zeta_{csa}$.
[f]$\Omega = |\delta_{33} - \delta_{11}|$.
[g]$\kappa = 3(\delta_{22} - \delta_{iso})/\Omega$.

Table III. NMR Properties of Mercury Halide Nuclei[a]				
Isotope	Spin	Natural Abundance (%)	Magnetogyric Ratio ($\gamma/10^7$ rad s^{-1} T^{-1})	Quadrupolar Moment (Q/fm^2)
^{199}Hg	1/2	16.87	4.8457916	--
^{201}Hg	3/2	13.18	-1.788769	38.6
^{19}F	1/2	100	25.18148	--
^{35}Cl	3/2	75.78	2.624198	-8.165
^{37}Cl	3/2	24.22	2.184368	-6.435
^{79}Br	3/2	50.69	6.725616	31.3
^{81}Br	3/2	49.31	7.249776	26.2
^{127}I	5/2	100	5.389573	-71.0
[a]From Ref. 9				

Table IV. Atomic Distances in Mercurous(I) Halides				
Compound	Hg-Hg Bond Length[a] (pm)	Hg-Hg Bond Length[b] (pm)	Hg-X Bond Length[a] (pm)	Hg-X Bond Length[b] (pm)
Hg_2F_2	243	250.7	231	2 x 214
			4 x 270	4 x 271.5
Hg_2Cl_2	253	252.6	---	2 x 243
				4 x 320.9
Hg_2Br_2	258	249	---	2 x 271
				4 x 332
Hg_2I_2	269	---	---	---
[a]From Ref. 46 [b]From Ref. 47				

Figures

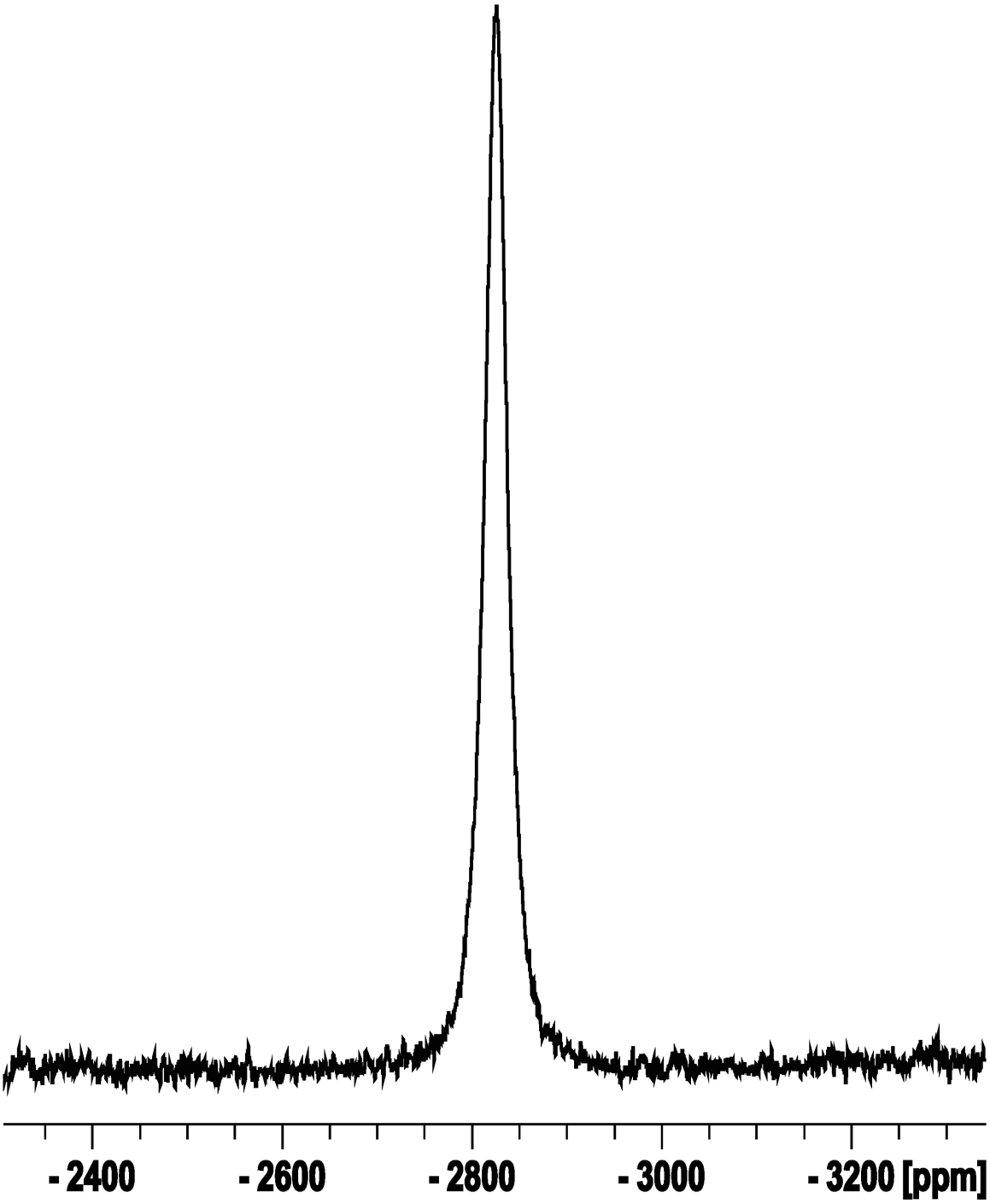

Figure1: ^{199}Hg NMR of a static sample of polycrystalline HgF_2.

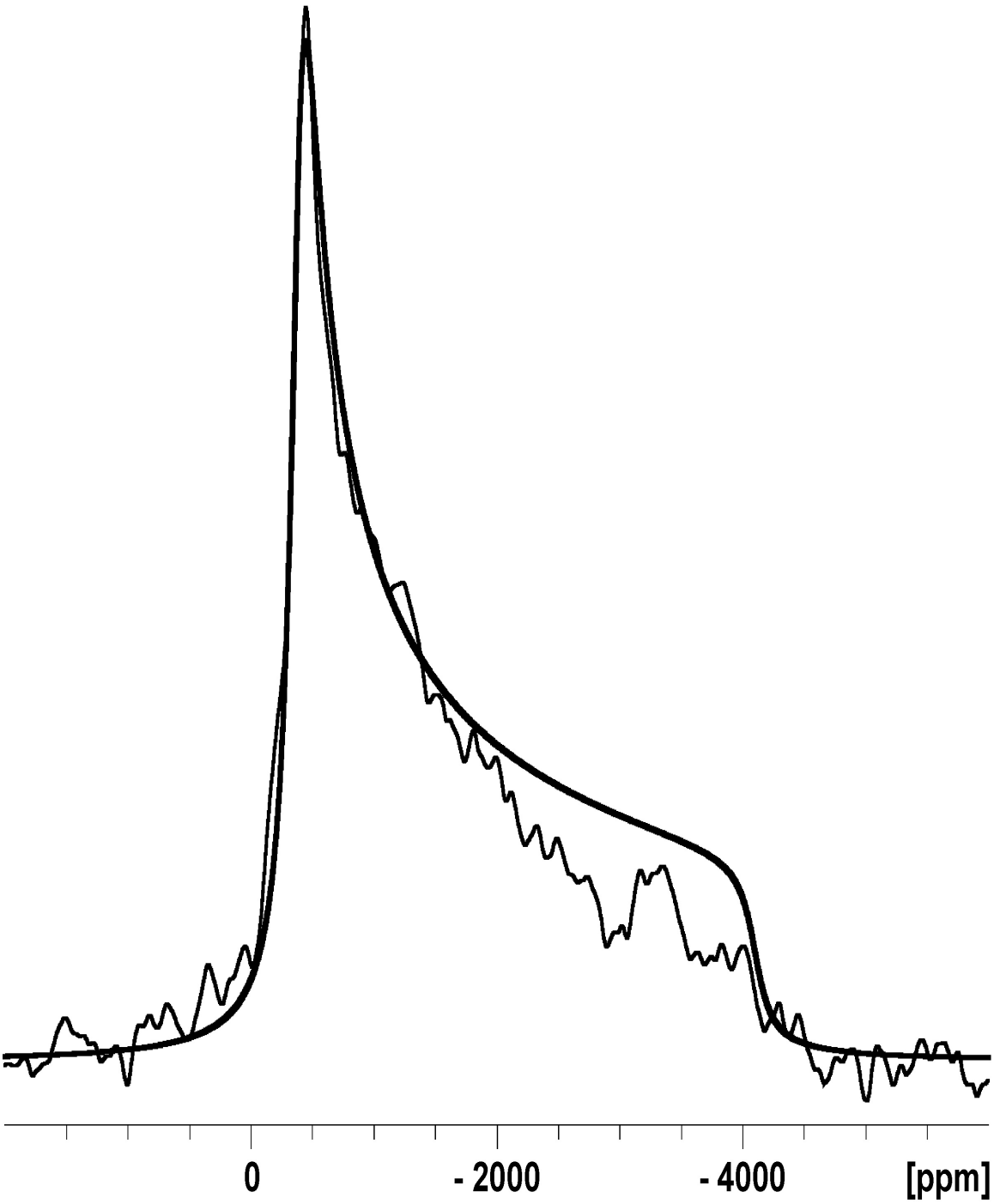

Figure 2: ^{199}Hg VOCS NMR spectrum of a static sample of polycrystalline $HgCl_2$. The smooth line is a simulation to extract the CSA principal values.

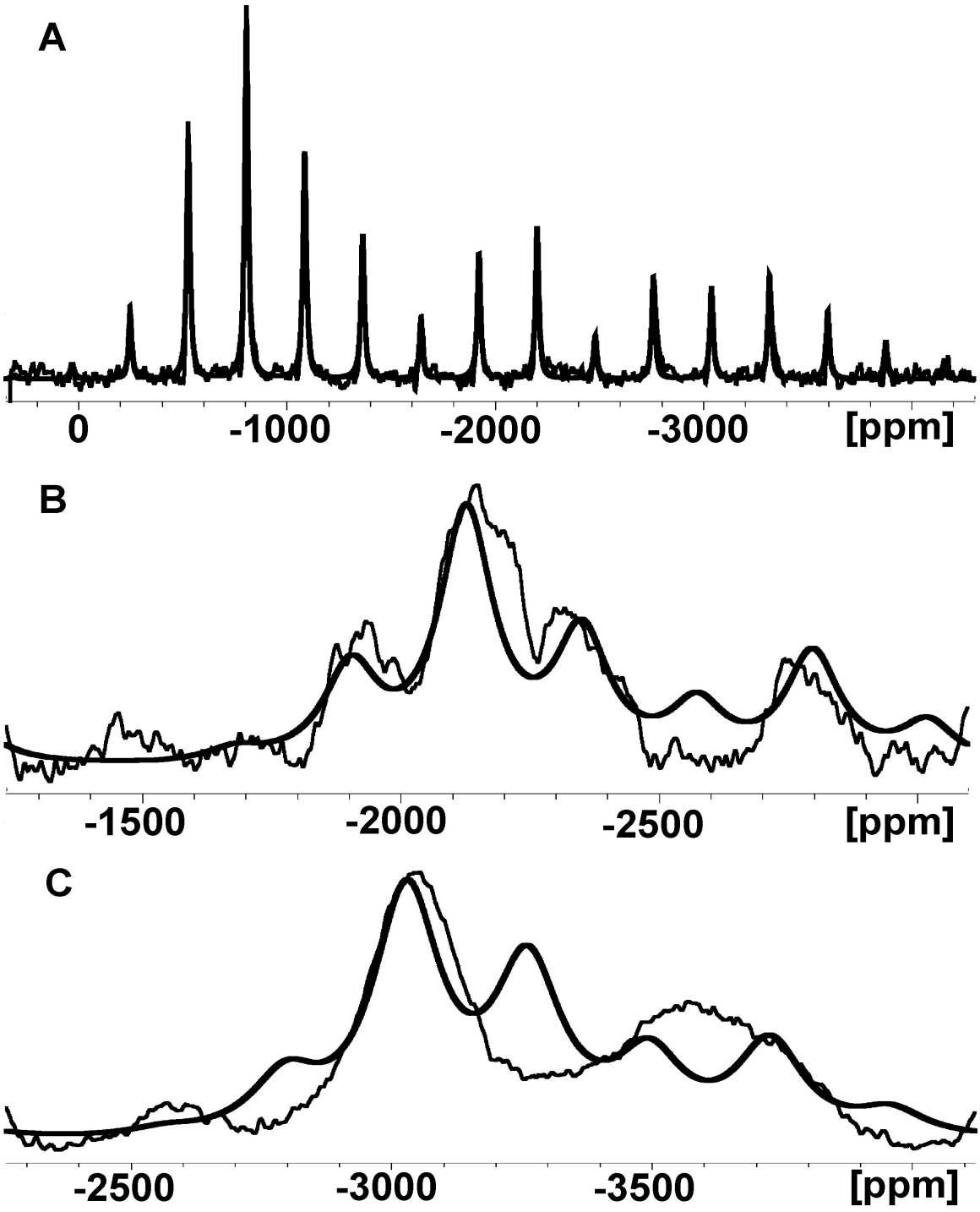

Figure 3: The ^{199}Hg MAS spectra of (A) polycrystalline $HgCl_2$ acquired with a rotation speed of 15 kHz, (B) polycrystalline $HgBr_2$ acquired with a rotation speed of 12 kHz, and (C) polycrystalline HgI_2 acquired with a rotation speed of 12.5 kHz. The smooth lines in each are Herzfeld-Berger simulations to extract the CSA principal values. This method of analysis fails as the size of the quadrupolar coupling constant of the halide becomes larger (see text).

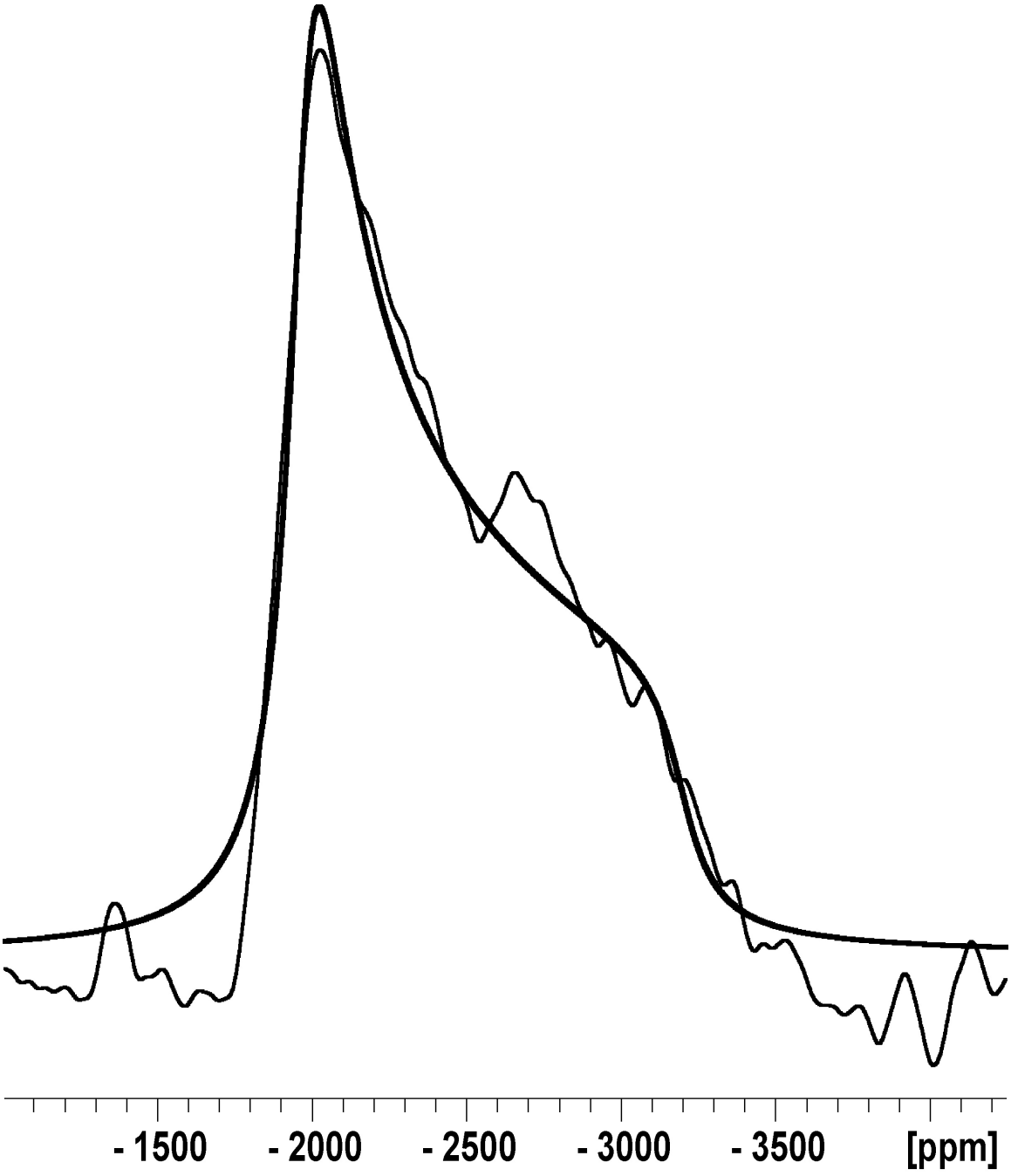

Figure 4: ^{199}Hg VOCS NMR spectrum of a static sample of polycrystalline $HgBr_2$. The smooth line is a simulation to extract the CSA principal values.

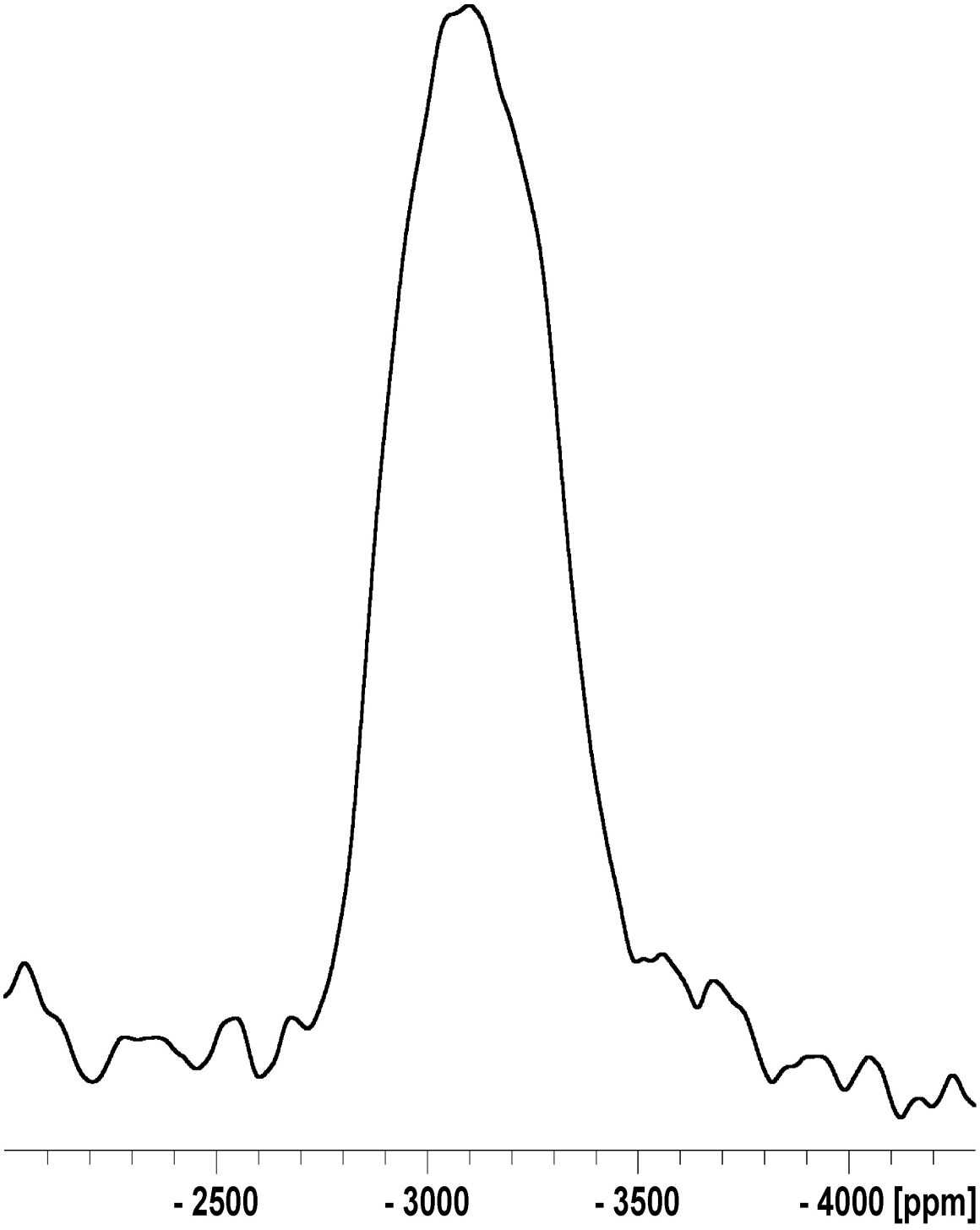

Figure 5: ^{199}Hg VOCS NMR spectrum of a static sample of polycrystalline HgI_2.

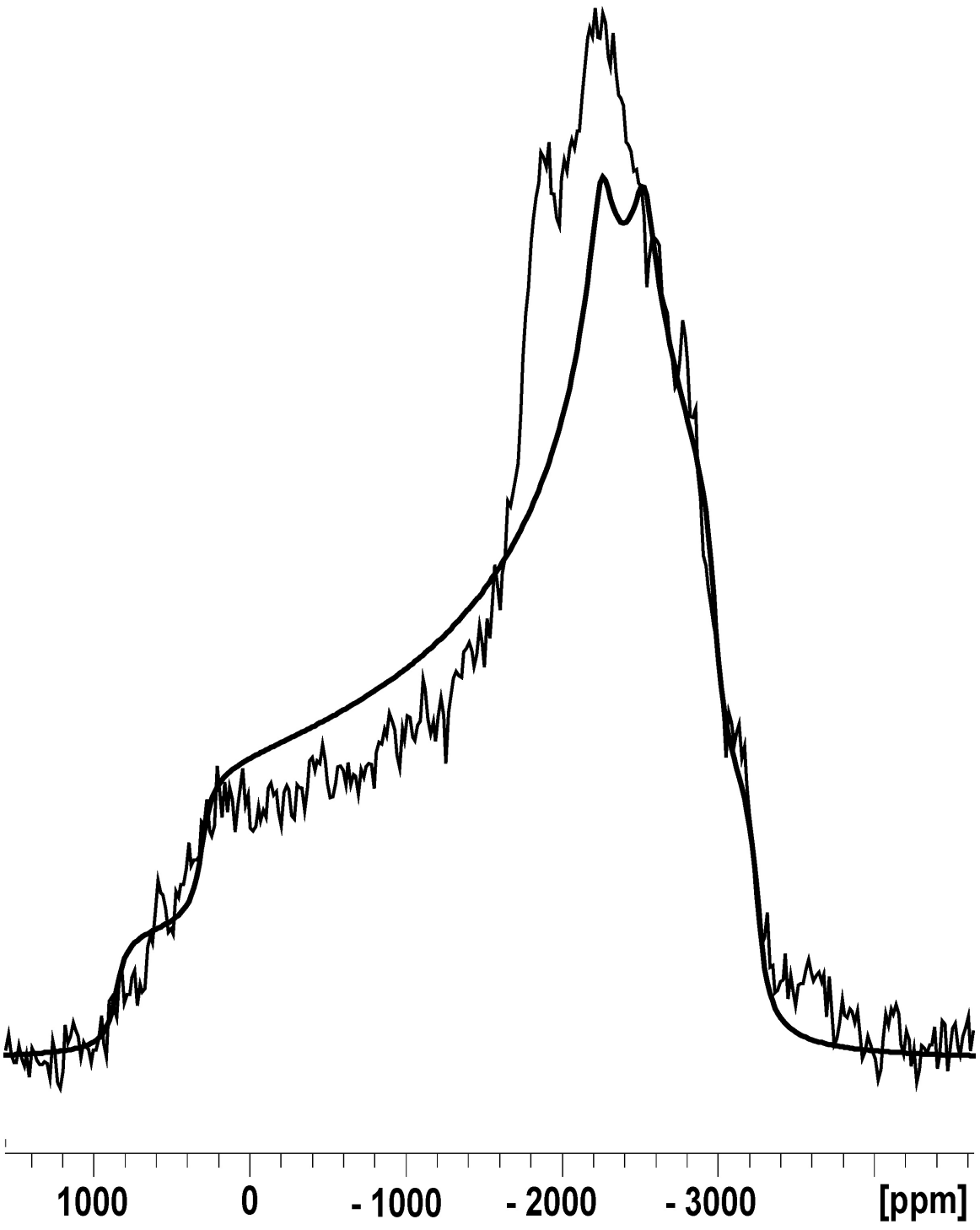

Figure 6: ^{199}Hg NMR spectrum of a static sample of polycrystalline Hg_2F_2. The smooth line is a simulation of the CSA tensor with a co-linear heteronuclear dipolar interaction (see text).

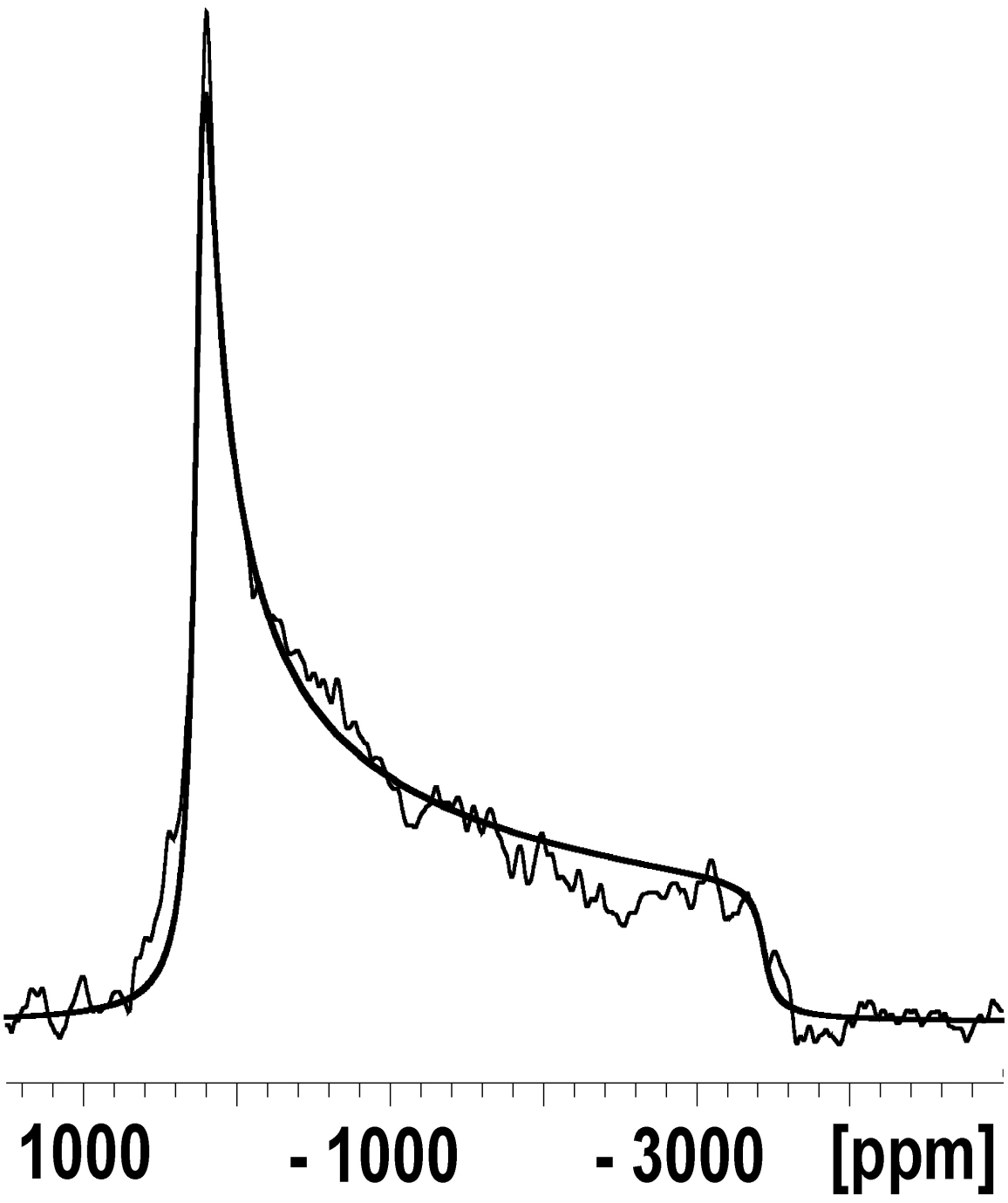

Figure 7: ^{199}Hg VOCS NMR spectrum of a static sample of polycrystalline Hg_2Cl_2. The smooth line is a simulation to extract the CSA principal values.

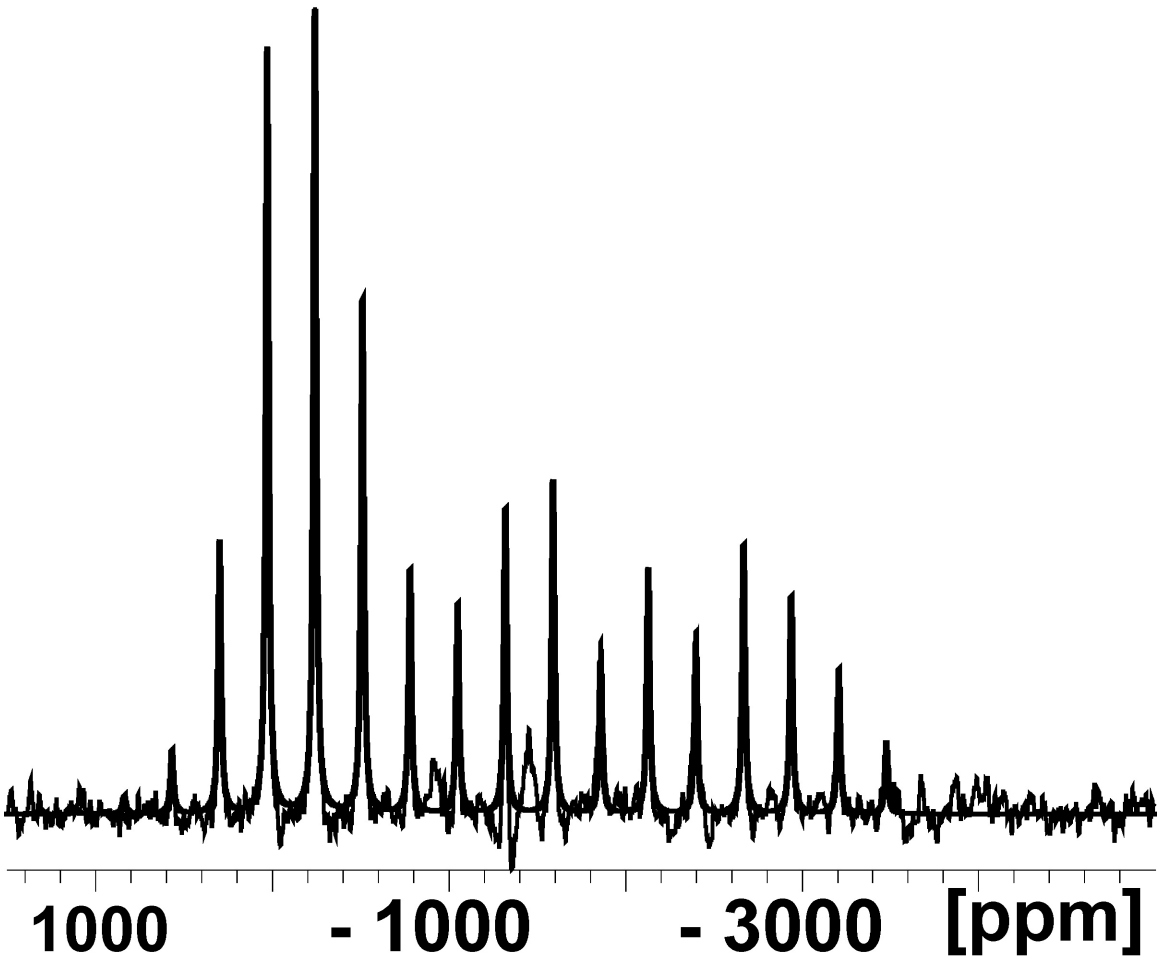

Figure 8: ^{199}Hg MAS spectrum of a sample of polycrystalline Hg_2Cl_2 acquired with a rotation speed of 14.5 kHz. The smooth line is a simulation to extract the CSA principal values.